ACS APPLIED MATERIALS & INTERFACES

Research Article

www.acsami.org

Substrate Stiffness Together with Soluble Factors Affects Chondrocyte Mechanoresponses

Cheng Chen,*[,†] Jing Xie,[‡] Linhong Deng,[§] and Liu Yang*[,†]

[†]Center for Joint Surgery, Southwest Hospital, Third Military Medical University, Chongqing 400038, China

[‡]State Key Laboratory of Oral Diseases, West China Hospital of Stomatology, Sichuan University, Chengdu, Sichuan 610064, China

[§]Institute of Biomedical Engineering and Health Sciences, Changzhou University, Changzhou, Jiangsu 213164, China

ABSTRACT: Tissue cells sense and respond to differences in substrate stiffness. In chondrocytes, it has been shown that substrate stiffness regulates cell spreading, proliferation, chondrogenic gene expression, and TGF-β signaling. But how the substrate stiffness together with soluble factors influences the mechanical properties of chondrocyte is still unclear. In this study, we cultured goat articular chondrocytes on polyacrylamide gels of 1, 11, and 90 kPa (Young's modulus), and measured cellular stiffness, traction force, and response to stretch in the presence of TGF-β1 or IL-1β. We found that TGF-β1 increased cellular stiffness and traction force and enhanced the response to stretch, while IL-1β increased cellular stiffness, but lowered traction force and weakened the response to stretch. Importantly, the effects of TGF-β1 on chondrocyte mechanics were potent in cells cultured on 90 kPa substrates, while the effects of IL-1β were potent on 1 kPa substrates. We also demonstrated that such changes of chondrocyte mechanoresponse were due to not only the changes of actin cytoskeleton and focal adhesion, but also the alteration of chondrocyte extracellular matrix synthesis. Taken together, these results provide insights into how chondrocytes integrate physical and biochemical cues to regulate their biomechanical behavior, and thus have implications for the design of optimized mechanical and biochemical microenvironments for engineered cartilage.

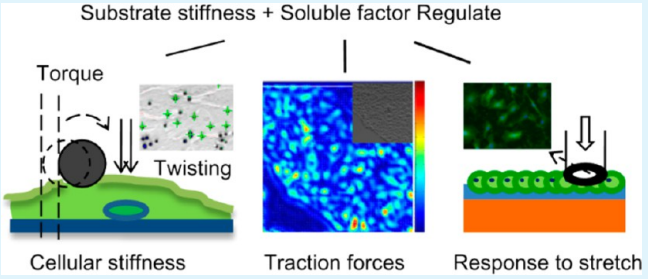

KEYWORDS: *substrate stiffness, chondrocyte, actin, focal adhesion, traction force, stretch*

1. INTRODUCTION

Tissue cells sense and respond to physical cues from the extracellular environment. These physical cues include topography,[1] gradient,[2] roughness,[3] thickness,[4] and elasticity[5] of the extracellular matrix (ECM). Among them, ECM elasticity is of particular interest because it has been shown to play fundamental roles in regulating diverse aspects of cell behaviors.[6] For example, a stiffer ECM generally increases cellular stiffness, promotes cell adhesion and spreading, and upregulates cell proliferation.[7] ECM elasticity also regulates cell migration, as adherent cells tend to migrate from soft regions to stiff regions of the ECM.[8] Moreover, ECM elasticity even regulates stem cell fate and differentiation.[9] All these findings provide valuable insights to cell biology, tissue engineering, and regenerative medicine. Substrates with physiological stiffness are beginning to replace the long-term use of traditional tissue-culture plastic in cellular experiments in vitro; also, in tissue engineering, the elasticity of scaffold has been regarded as a key parameter in maintaining cellular phenotype or directing stem cell differentiation.

In cartilage tissue engineering, it is found that the cartilage cell—chondrocyte—progressively loses its chondrogenic phenotype[10] during in vitro expansion on a hard culture dish with a stiffness in the gigapascal range, which directly affects the efficiency of cartilage repair. Therefore, to maintain the chondrocyte phenotype, compliant natural hydrogels such as alginate,[11] agarose,[12] and collagen[13] have been used as alternative cell culture substrates. However, natural gels have a limited tailorability of mechanical properties; thus they are not good choices in investigating chondrocyte mechanosensing to substrates that require precisely controlled stiffness. In this case, synthetic hydrogels with excellent tunability of elasticity are more suitable.[14] One well-established synthetic hydrogel is polyacrylamide (PA), which has been proved as a classic model to study cell–substrate interaction.[15] Although PA substrates have been widely used in many cell types, their applications on chondrocytes are comparatively few. Schuh et al. found that chondrocytes have a decreased spreading, proliferation, and F-actin level but a higher expression of type II collagen and aggrecan on PA gel of 4 kPa compared to gels of 10, 40, and 100 kPa.[16] Allen et al. showed that the expression of chondrogenic marker genes Sox9, Col2α1, and aggrecan is higher in chondrocytes on 0.5 MPa PA gel than on 1.1 and 0.2 MPa gel; moreover, exogenous transforming growth factor β (TGF-β) exhibits better chondrogenic effects on 0.5 MPa gel than on plastic.[17]

Received: June 25, 2014
Accepted: August 27, 2014
Published: August 27, 2014

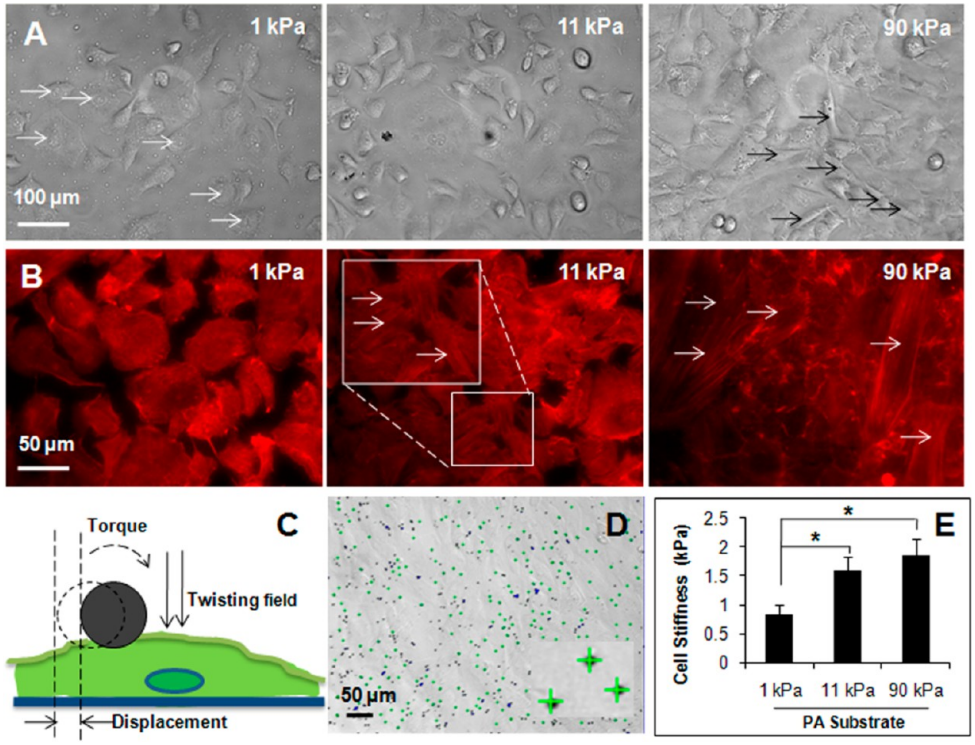

Figure 1. Effects of substrate stiffness on chondrocyte morphology, stress fiber assembly, and cellular stiffness. (A) Phase contrast images of chondrocytes cultured on PA substrates 6 days after seeding. White arrows point to polygonal cells; black arrows point to elongated cells. (B) Stress fiber formation of chondrocytes cultured on PA substrates for 6 days. Cells were stained with phalloidin (red) for actin filaments. White arrows point to stress fibers. (C) Schematic of optical magnetic twisting cytometry (OMTC) for probing cellular stiffness. (D) Typical micrograph showing magnetic microbeads adhered to chondrocytes during OMTC measurement. The green crosses indicate real-time tracking of bead centroids. (E) Young's modulus of chondrocytes cultured on PA substrates. Data were presented as mean ± standard deviation (SD) for total ≥528 magnetic microbeads from three independent experiments (*, $p < 0.05$).

These studies serve as a good example of PA substrates with varying stiffness impacting chondrocyte biology. However, the biomechanical behavior of chondrocytes in response to varying substrate stiffness remains unknown. Mechanical factors including substrate stiffness are of importance because both the abnormal responses to mechanical signals and the responses to abnormal mechanical signals lead to pathological changes of chondrocytes.[18] Besides the regulation of mechanical factors, the regulation of chondrocytes to soluble factors (growth factors, cytokines, chemokines) is also extremely crucial since there is no cell−cell communication in cartilage. Therefore, to study chondrocyte biomechanics in the presence of soluble factors, in this study we focused on the mechanoresponses of chondrocyte cytoskeleton and focal adhesion on PA substrates with differing stiffness. We investigated the actin cytoskeleton dynamics through measuring cellular stiffness and the cell−substrate adhesion dynamics through measuring cell traction forces. We also measured the responses of chondrocyte stiffness and traction force to varying substrate stiffness in the presence of TGF-β1 that induces anabolic effects or interleukin-1β (IL-1β) that induces catabolic effects on chondrocyte matrix. Finally, we tested the changes of chondrocyte actin cytoskeleton and vinculin focal adhesion when the PA substrates were subjected to a mechanical stretch.

2. MATERIALS AND METHODS

2.1. Fabrication of PA Substrates. PA gel substrates were prepared according to our previous protocol with minor modifications.[19] The glass bottom of the 35 mm dishes (P25-G-020-C, MatTek Corp., Ashland, MA) was treated with bind silane to facilitate gel attachment. Then, 300 μL of a gel solution containing acrylamide (Bio-Rad, Hercules, CA) and bis-acrylamide (Bio-Rad) of different volume concentrations (Young's modulus at 1 kPa, 5% acrylamide and 0.03% bis-acrylamide; at 11 kPa, 10% acrylamide and 0.07% bis-acrylamide; at 90 kPa, 12% acrylamide and 0.3% bis-acrylamide), 5% ammonia persulfate (Bio-Rad), and 0.05% TMMED (Bio-Rad) was added to the center of the glass bottom of each dish and covered by a 25 mm circular coverslip (VWR) to yield a gel with a final thickness of ~700 μm. After gel polymerization, the coverslips were gently removed with a forceps, and gels were surface-activated using sulfosuccinimidyl-6-[4-azido-2-nitrophenylamino]hexanoate (Sulfo-SANPAH; Pierce, Rockford, IL) under UV light for 10 min. These gel substrates were then coated with type I collagen (0.1 mg/mL in phosphate-buffered saline (PBS); Advanced BioMatrix, San Diego, CA) and stored overnight at 4 °C. On the next day, the collagen solution was removed from the gels, and the gels were kept in PBS at 4 °C until use. In particular, to prepare gel substrates for cell traction measurement, 0.6% (v/v) of 0.5 μm diameter pink fluorescent beads (Invitrogen, Eugene, OR) were added into the gel solution.

2.2. Cell Isolation and Culture. Chondrocytes were isolated based on a previous protocol[20] with modifications. Cartilage specimens were harvested from healthy knee joints of Spanish goats. Specimens were washed thoroughly in PBS supplemented with 1% (v/v) penicillin/streptomycin (P/S; Life Technologies) and then diced to less than a millimeter in size. Chondrocytes from the diced tissues were isolated by digesting the matrix overnight in advanced Dulbecco's modified Eagle's medium (ADMEM; Gibco, Life Technologies) supplemented with 400 U/mL type II collagenase (Worthington Biochemical, Lakewood, NJ), 10% (v/v) fetal bovine serum (FBS; Hyclone Technologies, Logan, UT), and 1% P/S. The resulting cell suspension was filtered through a 40 μm cell strainer; collected cells were washed by centrifugation and resuspended in ADMEM supplemented with10% FBS, 1% P/S, 1 ng/mL TGF-β1 (R&D

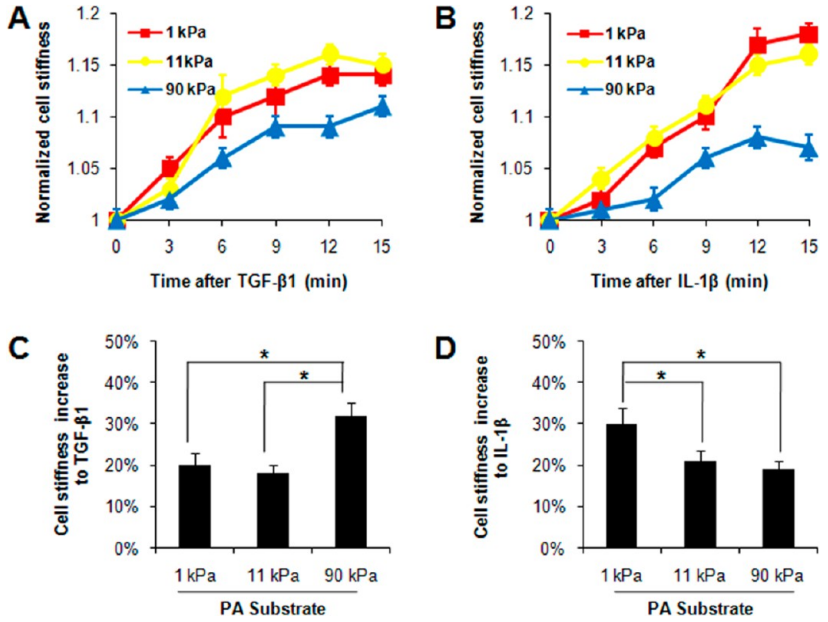

Figure 2. Effects of TGF-β1 and IL-1β on the stiffness of chondrocytes cultured on 1, 11, and 90 kPa PA substrates. (A, B) Real-time responses of chondrocyte stiffness to (A) TGF-β1 and (B) IL-1β within 15 min. Cellular stiffness of each cell was normalized to its own value before drug intervention. (C, D) Increased percentage of chondrocyte stiffness after 1 day treatment of (C) TGF-β1 and (D) IL-1β. Data were presented as mean ± SD for total ≥573 magnetic microbeads from three independent experiments (*, $p < 0.05$).

Systems, Minneapolis, MN), 5 ng/mL fibroblast growth factor-2 (FGF-2; R&D Systems), and 10 ng/mL platelet-derived growth factor $\beta\beta$ (PDGF-$\beta\beta$; R&D Systems). Upon reaching ~80% confluence, cells were released from the flask by trypsinization and plated onto the gel substrates at a density of 2500 cells/cm^2 (unless otherwise noted) in ADMEM supplemented with10% FBS, 1% P/S, and 0.1 mM ascorbic acid 2-phosphate (Sigma-Aldrich, St. Louis, MO). The medium was changed every 2 days.

Six days after cell seeding, the concentration of FBS in the culture medium was reduced from 10 to 1% to minimize the compounding effects of soluble factors. Then, 10 ng/mL TGF-β1 or 10 ng/mL IL-1β (R&D Systems) was added to chondrocytes in experimental groups. Cell responses were measured immediately or after 24 h.

2.3. Measurement of Cellular Stiffness. The stiffness of chondrocytes was probed using optical magnetic twisting cytometry (OMTC).[21,22] First, ferrimagnetic beads (4.5 μm diameter, fabricated in Dr. Jeffery Fredberg's lab in the Harvard School of Public Health, Boston, MA) were coated with a peptide containing the sequence Arg-Gly-Asp (150 μg of ligand/mg of microbeads) overnight in carbonate buffer. The next day, these beads were incubated with cells for 20 min to allow the beads to bind to cell surface receptors that link to the underlying cytoskeleton. Then, a gel dish was mounted to a microscope stage equipped with a bead twisting setup. The beads were magnetized horizontally and then twisted in an oscillatory magnetic field with a frequency of 0.75 Hz. This exerted a sinusoidal torque that caused the beads to twist, with resulting back-and-forth horizontal translation (Figure 1C). The motions of beads were recorded with a Leica DMIRB CCD camera (Figure 1D). The specific torque (T) applied to a bead was computed as $T = mB/V$, where V is the bead volume, m is the bead magnetic moment, and B is the applied magnetic field. The complex elastic modulus (G^*) of the cell was computed from the Fourier transforms of the applied torque T^* and of the resulting bead displacement (d^*), as given by $G^* = T^*/d^* = G' + jG''$, where G' is the storage modulus, which we referred to as cellular stiffness (in pascals per nanometer), G'' is the loss modulus, and $j^2 = -1$. OMTC is a highly localized measurement, as it has been shown in a study using finite element modeling that the stress induced by the torque (T) decays rapidly in the radial direction as a function of $1/r^3$, where r is the distance from the bead surface; within one bead diameter (4.5 μm), the stress would become quite small (~1%).[23] Taking into account the chondrocyte thickness (~5 μm)[24] and extent of bead imbedding (30−40% at the cell surface), the computed results of cellular stiffness in our study were not affected by the substrate, and a length scale[25] of 1300 nm was multiplied to the real component G' to get the Young's modulus of chondrocytes. A custom Matlab script recorded the position of all tested beads every 4 s during the OMTC measurement. For calculation of baseline cellular stiffness, data obtained from a 20 s time course OMTC measurement were used; for calculation of changes of cellular stiffness upon TGF-β1 or IL-1β treatment, a 15 min time course OMTC measurement was carried out.

2.4. Traction Force Microscopy. Gel substrates embedded with fluorescent beads were used in traction force microscopy.[26] Using a Leica DM6000 B microscope, the positions of fluorescent beads were recorded at the pretreatment baseline, at 30, 60, 90, 120, 150, and 180 min following TGF-β1 or IL-1β treatment, and after detaching the cells by trypsinization at the end of the experiment. We used Fourier transform traction cytometry (FTTC)[27] to compute the constrained traction field. From the constrained traction field, we extracted the root-mean-square traction (RMST),[27,28] which is a scalar measure of the cell's net contractile strength. For single cell traction, low cell seeding density (1250 cells/cm^2) was adopted to avoid interference from adjacent cells; for monolayer traction, 2 mm diameter polydimethylsiloxane (PDMS) patterning[29] was used to confine the confluent chondrocyte monolayer in specific circular regions.

2.5. Immunofluorescence. Cells were fixed in 4% paraformaldehyde in PBS for 15 min and permeabilized in PBS containing 0.25% Triton X-100 (Sigma-Aldrich) for 10 min. Nonspecific bindings were blocked with 1% bovine serum albumin (BSA; Sigma-Aldrich) in PBS for 30 min. For F-actin, fixed cells were stained with Alexa 594 Phalloidin (Molecular Probes) for 30 min at room temperature. For vinculin, fixed cells were incubated with mouse antivinculin primary antibody (1:100, Sigma-Aldrich) for 1 h at room temperature and Alexa 488 donkey antimouse secondary antibody (1:400 dilution, Abcam) for another 1 h at room temperature in the dark. For type II collagen and aggrecan, cells were incubated with rabbit anticollagen II (1:200, Abcam) and mouse antiaggrecan (1:200, Abcam), respectively, overnight and then incubated with Alexa 594 goat antirabbit secondary antibody (1:500, Molecular Probes) and Alexa 488 donkey antimouse secondary antibody (1:500, Abcam) for 1 h, respectively. Nuclei were stained with 0.1 μg/mL 4′,6-diamidino-2-phenylindole (DAPI; Sigma-Aldrich) in PBS for 1 min. Immunostained preparations were observed with a Leica DM 6000 B microscope with a 20× or 10× objective.

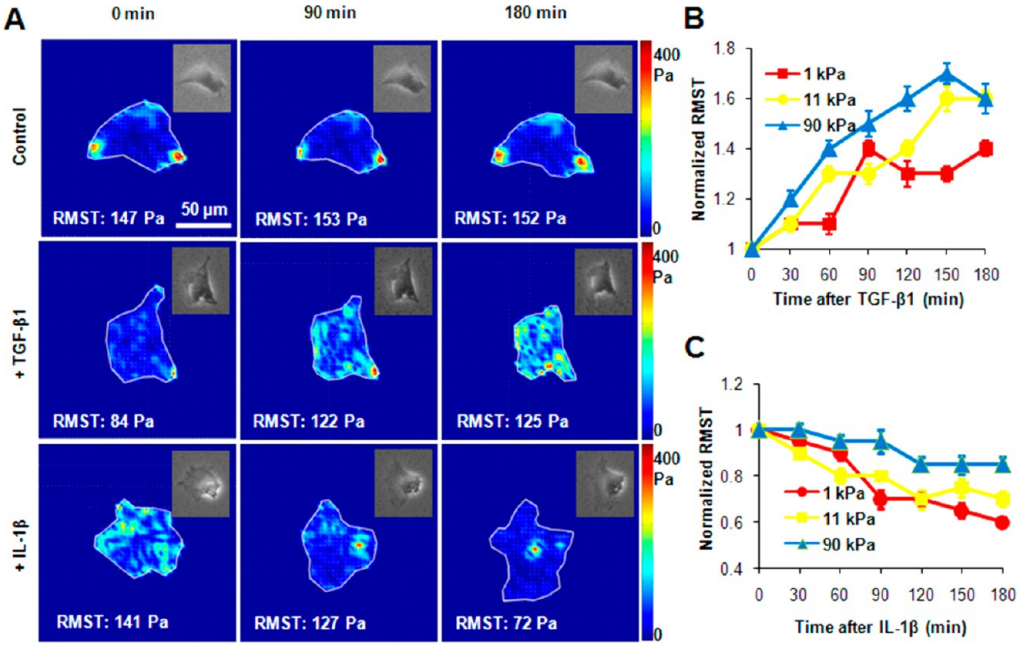

Figure 3. Effects of TGF-β1 and IL-1β on traction forces of single chondrocyte cultured on 1, 11, and 90 kPa PA substrates. (A) Traction maps of single chondrocytes on 11 kPa substrates at 0, 90, and 180 min of drug intervention (top, control; middle, TGF-β1; bottom, IL-1β; insets, phase contrast images of chondrocytes during measurement). (B, C) Responses of RMST to (B) TGF-β1 and (C) IL-1β within 180 min. RMST of each cell was normalized to its own value before drug intervention. Data were presented as mean ± SD (n = 4; ∗, p < 0.05).

Images were acquired using Leica Application Suite Advanced Fluorescence (LAS AF). To quantify the intensity of stained actin and vinculin, at least three staining images for each experimental group were analyzed using ImageJ. The intensity of actin or vinculin was calculated by dividing the intensity of a chosen field by the number of cells within (determined by the number of stained nucleus).

2.6. Stretch Apparatus. An improved custom-built stretch setup was used.[19,30] Briefly, a biaxial strain was imposed by lowering a hollow circular punch indenter (inside diameter 2 mm, outside diameter 3 mm) onto the PA substrate. The indenting depth was controlled by a stepper motor through a customized Labview program. The magnitude of the strain was calibrated based on the displacement of fluorescent beads within the indenting region of the substrate, with an indenting depth of 450 μm yielding a 15% strain to the PA substrate. After indentation, the indenter was lifted, and the PA substrate recoiled elastically.

2.7. Statistical Analysis. All of the data were expressed as mean ± standard deviation (SD). A two-tailed Student t test was performed to determine the statistical significance between two groups. A value of p < 0.05 was considered statistically significant.

3. RESULTS

3.1. Substrate Stiffness Affected Chondrocyte Morphology, Actin Cytoskeleton, and Cellular Stiffness. The goat articular chondrocytes cultured on PA substrates with varying stiffness for 6 days showed different cell shapes (Figure 1A), with most polygonal cells on 1 kPa substrates and most elongated cells on 90 kPa substrates. Images of actin staining (Figure 1B) showed that, with the increase of substrate stiffness, chondrocytes exhibited an increased amount of stress fibers (SFs). On 1 kPa substrates, SFs were barely seen; on 11 kPa substrates, moderate SFs were visible; on 90 kPa substrates, prominent parallel SFs were formed. The stiffness of the PA substrate also influenced chondrocyte stiffness (Figure 1E). The Young's modulus of chondrocytes (E_{chon}) measured with OMTC was 0.83 ± 0.16 kPa on 1 kPa substrates, significantly lower than those of chondrocytes on 11 kPa substrates (E_{chon} = 1.59 ± 0.23 kPa) and 90 kPa substrates (E_{chon}= 1.86 ± 0.27 kPa). All these results indicated chondrocytes perceived the difference of substrate stiffness and responded differently.

3.2. Changes of Chondrocyte Stiffness to TGF-β1 or IL-1β. To investigate if the effects of TGF-β1 and IL-1β on chondrocytes were affected by substrate stiffness, we measured the real-time responses of cellular stiffness upon TGF-β1 or IL-1β exposure and the changes of cellular stiffness after 1 day of treatment of TGF-β1 or IL-1β. Chondrocytes responded to either TGF-β1 (Figure 2A) or IL-1β (Figure 2B) promptly, as indicated by the immediate increase of cellular stiffness. Within 15 min of TGF-β1 or IL-1β addition, chondrocytes on PA substrates showed slightly different rates of increasing stiffness, with chondrocytes on 1 and 11 kPa substrates having similar trends and chondrocytes on 90 kPa substrates having a relatively slower increase rate of cellular stiffness. After 1 day of treatment of TGF-β1 (Figure 2C), chondrocytes on 90 kPa substrates showed 32 ± 3% increase in cellular stiffness, much higher than the stiffness increase of chondrocytes on 1 and 11 kPa substrates (both ∼20%). By contrast, after 1 day of treatment of IL-1β (Figure 2D), chondrocytes showed the biggest increase of cellular stiffness (30 ± 4%) on 1 kPa substrates and ∼20% increase of cellular stiffness on 11 and 90 kPa substrates. Taken together, chondrocytes showed a quicker immediate increase of stiffness in response to either TGF-β1 or IL-1β on 1 and 11 kPa substrates than on 90 kPa substrates, but the extent of stiffness increase after 1 day of treatment was different, with the biggest increase of chondrocyte stiffness induced by TGF-β1 and IL-1β occurring on 90 and 1 kPa substrates, respectively.

3.3. Traction Force of Single Chondrocyte in Response to TGF-β1 or IL-1β. To further study the effects of TGF-β1 and IL-1β on the mechanoresponses of chondrocytes, we monitored changes of the cell's traction force. A nontreated chondrocyte grown on 11 kPa substrate (control in Figure 3A, top panel) showed steady cellular

dx.doi.org/10.1021/am504135b | ACS Appl. Mater. Interfaces 2014, 6, 16106−16116

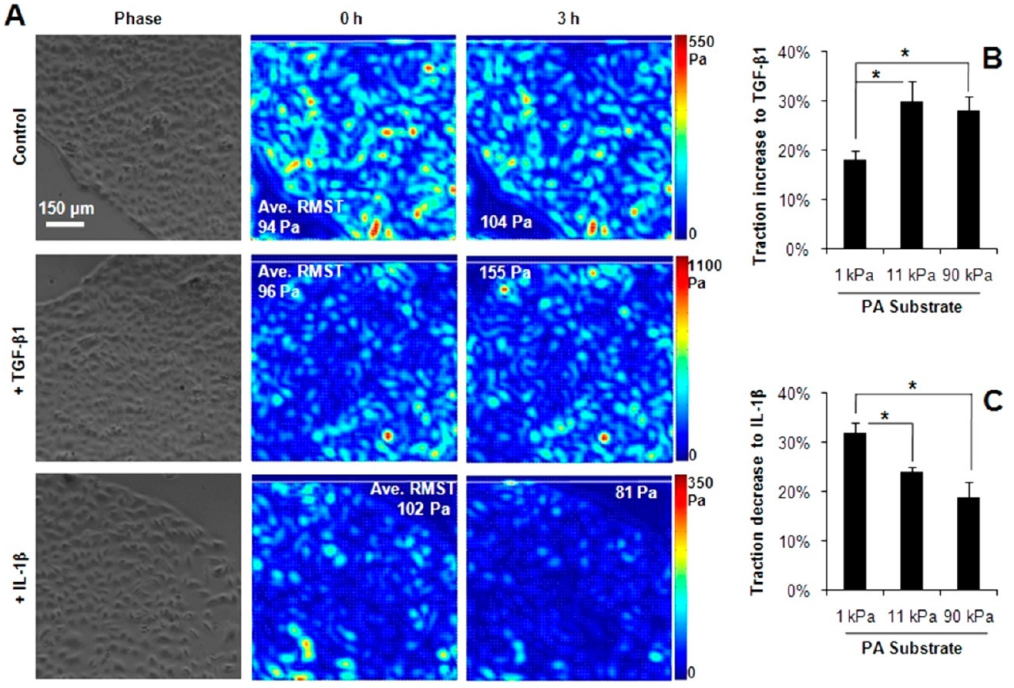

Figure 4. Effects of TGF- β1 and IL-1β on traction forces of chondrocyte monolayer cultured on 1, 11, and 90 kPa PA substrates. (A) Traction maps of chondrocyte monolayer on 11 kPa substrates before (0 h) and after 3 h treatment of TGF-β1 or IL-1β. (B) Increased percentage of chondrocyte monolayer RMST after 3 h of TGF-β1 treatment (n = 3; $*$, $p < 0.05$). (C) Decreased percentage of chondrocyte monolayer RMST after 3 h of IL-1β treatment. (n = 3; $*$, $p < 0.05$).

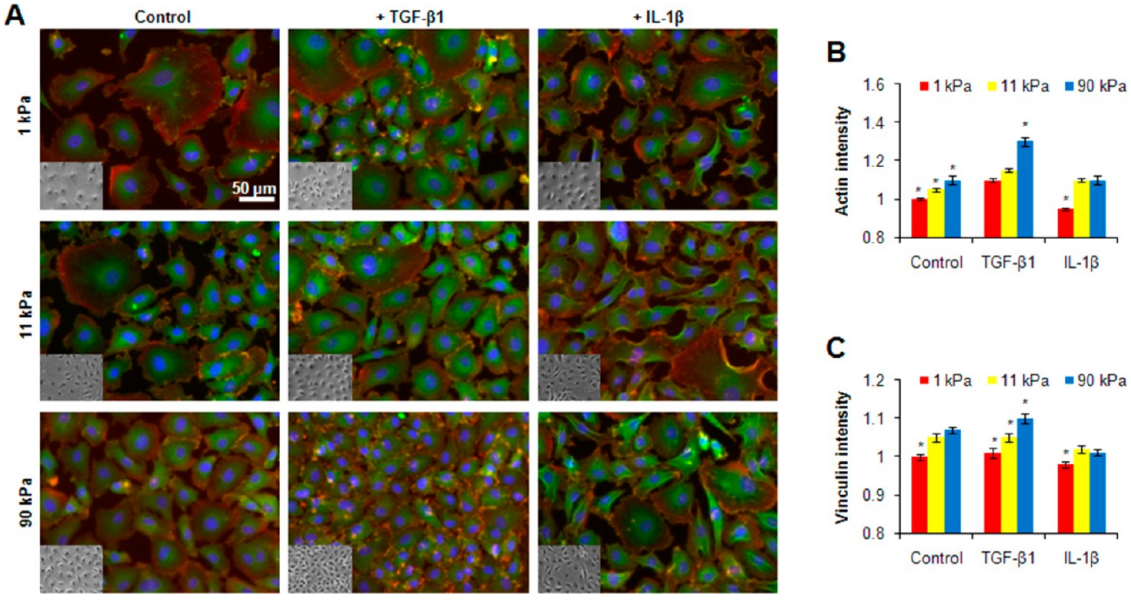

Figure 5. Fluorescence images showing staining of chondrocytes on 1, 11, and 90 kPa PA substrates, with or without 1 day treatment of TGF-β1 or IL-1β. (A) Cells were stained for actin (red), vinculin (green), and nuclei (blue). (insets) Phase contrast images of chondrocytes). (B, C) Quantified fluorescent level of (B) actin and (C) vinculin. Intensity was normalized to the intensity of actin or vinculin in untreated cells on 1 kPa substrates (n = 3; $*$, $p < 0.05$).

contractile strength (RMST at ~150 Pa) and the same traction force distribution (traction only localized at the leading corner and the trailing corner of the cell) during the 3 h observation. A TGF-β1 treated chondrocyte on 11 kPa substrate (Figure 3A, middle panel) showed increasing contractile strength (RMST from 84 to 125 Pa) and a broadening traction force distribution. On the contrary, an IL-1β treated chondrocyte on 11 kPa substrate (Figure 3A, bottom panel) showed decreasing contractile strength (RMST from 141 to 72 Pa) and a narrowing traction force distribution. Similar trends were also observed in single chondrocytes on 1 and 90 kPa substrates. Using the traction force of each single cell before drug treatment as its own control, we normalized the RMST after drug treatment. The results showed that single chondrocytes on 90 kPa substrates had the biggest increase in contractile strength to TGF-β1 (Figure 3B), whereas single chondrocytes

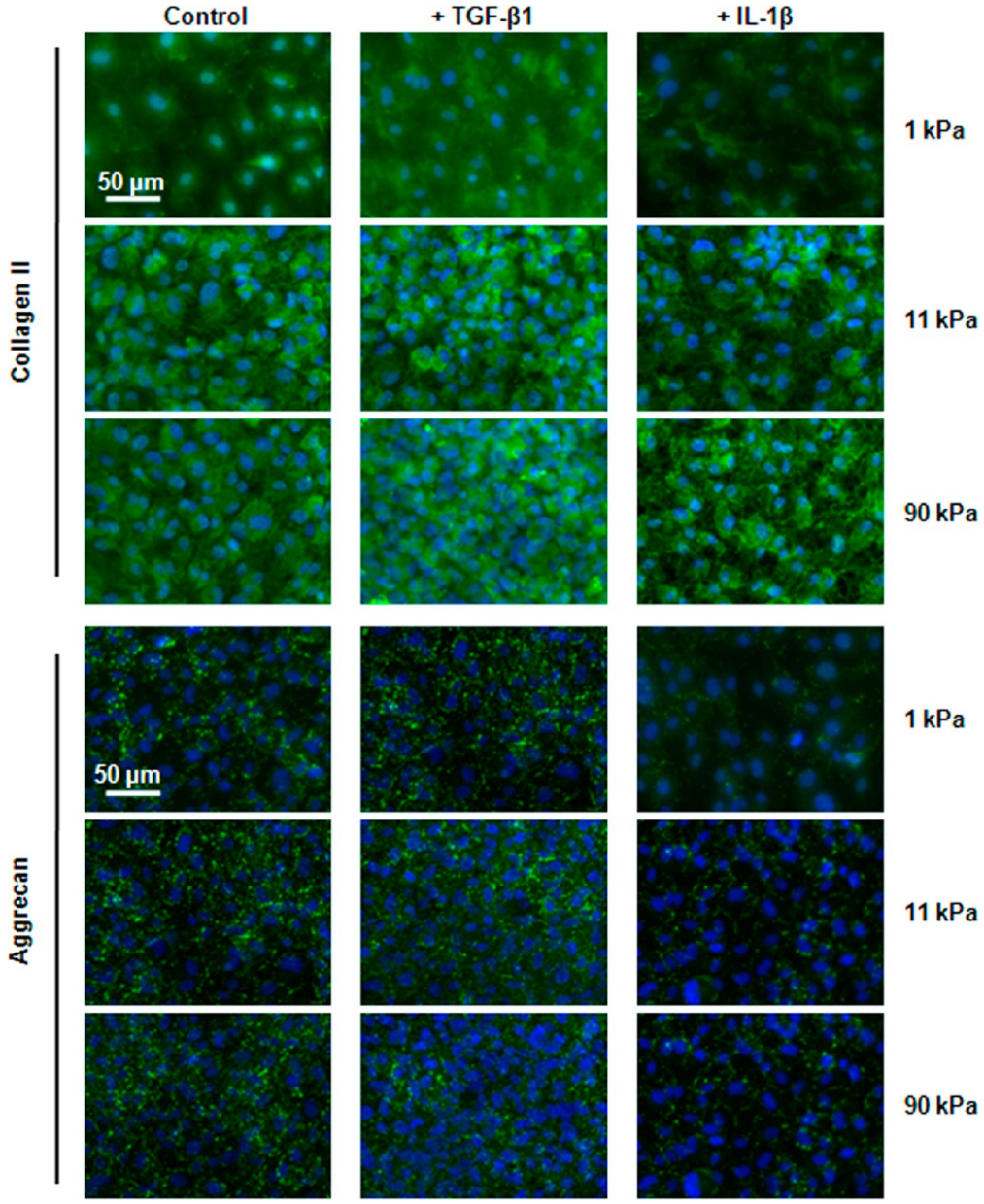

Figure 6. Fluorescence images showing type II collagen and aggrecan staining of TGF-β1 or IL-1β treated chondrocytes on 1, 11, and 90 kPa PA substrates. Cells were stained for type II collagen or aggrecan (green) and nuclei (blue).

on 1 kPa substrates had the biggest decrease in contractile strength to IL-1β (Figure 3C).

3.4. Traction Force of Chondrocyte Monolayer in Response to TGF-β1 and IL-1β. Single cells vary greatly in their ability to exert traction force due to different cell sizes, shapes, and locations. To further confirm the changes of cellular traction force due to TGF-β1 or IL-1β, we measured the traction force of a chondrocyte monolayer that consists of thousands of chondrocytes. Similar to single chondrocytes, during the 3 h real-time measurement, the average RMST of a chondrocyte monolayer on 11 kPa substrates remained stable if no drug was added (Figure 4A, top), increased in response to TGF-β1 (Figure 4A middle), but decreased in response to IL-1β (Figure 4A, bottom). We then quantified the percentage of traction force changes in chondrocyte monolayer. Results showed that, in response to TGF-β1 (Figure 4B), the chondrocyte monolayer on 1 kPa substrates exhibited an increase of traction force by 18 ± 2%, which was lower than the increase on 11 kPa (30 ± 4%) and 90 kPa substrates (28 ± 3%). In contrast, in response to IL-1β, the chondrocyte monolayer showed a higher decrease in traction force on 1 kPa substrates (32 ± 2%) as compared to 11 kPa (24 ± 1%) and 90 kPa substrates (19 ± 3%). Taking the single cell traction and monolayer traction force results together, we demonstrated that in general TGF-β1 increased whereas IL-1β decreased the traction force of the chondrocyte, and the effect on the cell traction force of TGF-β1 or IL-1β was potentiated toward either stiffer (90 kPa) or softer (1 kPa) substrates, respectively.

3.5. Changes of F-Actin and Vinculin to TGF-β1 and IL-1β. To help understand the mechanism of altering chondrocyte mechanosensing by TGF-β1 and IL-1β, here we visualized actin and vinculin in chondrocytes using fluorescence staining because the actin cytoskeleton is the main determinant of cellular stiffness, and vinculin focal adhesion is the main

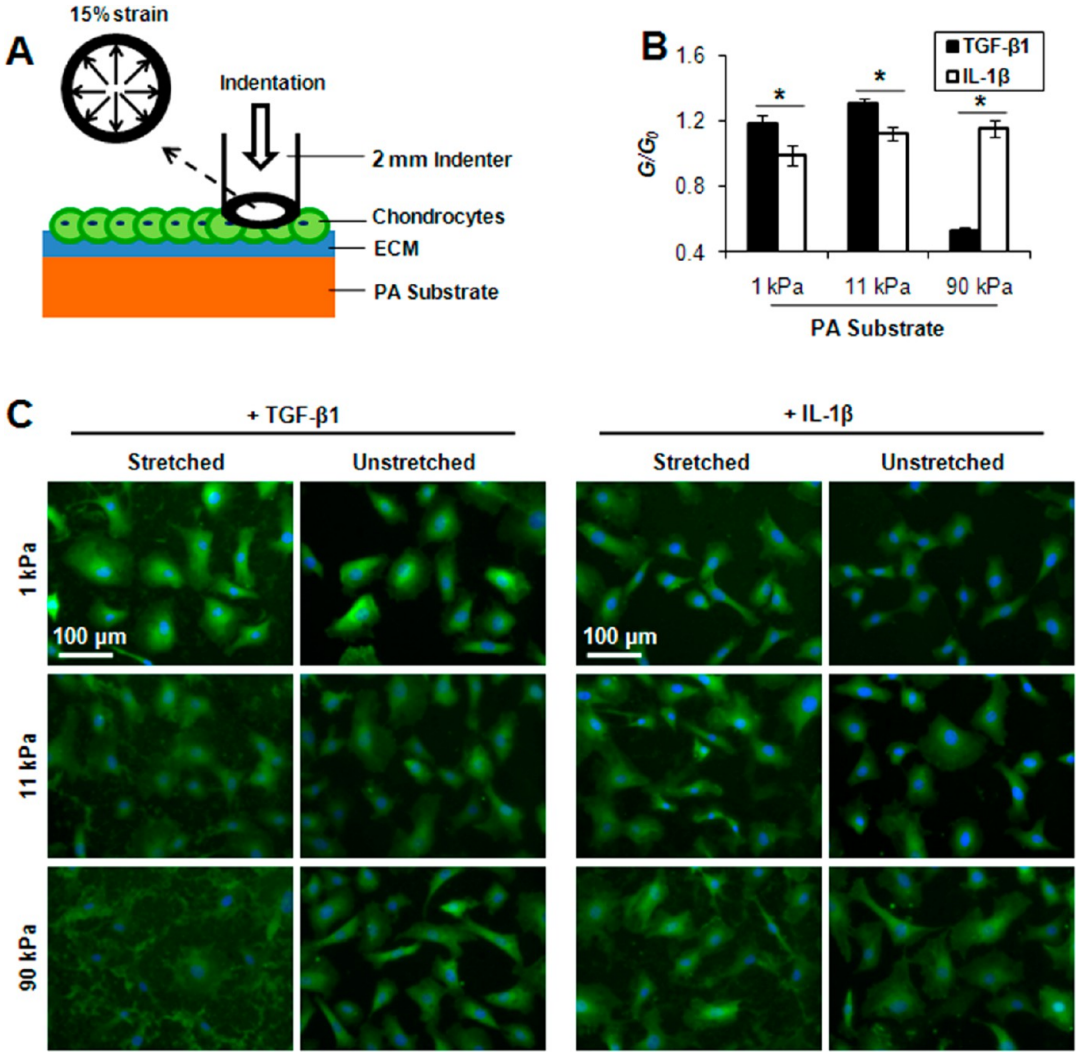

Figure 7. Effect of substrate stretch on chondrocytes. (A) Indentation induced biaxial strain to a circular region of PA substrate. (B) Changes of chondrocyte stiffness during stretch. The average cellular stiffness during a 30 s stretch (G) was normalized to stiffness of the same cells before stretch (G_0). (C) Fluorescence images showing vinculin staining of TGF-β1 or IL-1β treated chondrocytes in stretched and unstretched regions of 1, 11, and 90 kPa PA substrates (green, vinculin; blue, nuclei).

determinant of cell traction force. For nontreated chondrocytes (Figure 5B,C, control), the level of both actin and vinculin staining increased with increasing stiffness of the substrates. For TGF-β1 treated chondrocytes (Figure 5B,C, TGF-β1), the staining of actin appeared to be similar on 1 and 11 kPa substrates, but much stronger on 90 kPa substrates, while the staining of vinculin became stronger with increasing stiffness of substrate. For IL-1β treated chondrocytes (Figure 5B,C, IL-1β), the level of both actin and vinculin staining of chondrocytes on 1 kPa substrates was significantly weaker than that on 11 and 90 kPa. Moreover, IL-1β treated chondrocytes displayed obviously contracted cellular contours, suggesting not enough strength was provided by the substrate/ECM to resist the IL-1β induced contraction of chondrocytes. However, from the fluorescence intensity level of actin and vinculin, we could not explain why TGF-β1 and IL-1β had opposite effects on chondrocyte traction.

3.6. Changes of Chondrocyte ECM to TGF-β1 and IL-1β. To determine the effects of TGF-β1 and IL-1β on the ECM synthesis of chondrocytes on PA substrates, we stained the major ECM proteins: type II collagen and aggrecan (Figure 6). For nontreated chondrocytes, these proteins exhibited positive staining that became stronger on stiffer substrates. This indicated that chondrocytes deposited their own ECM on PA substrates, and the synthesis of ECM was promoted by increasing substrate stiffness from 1 to 90 kPa. In comparison, chondrocytes treated with TGF-β1 showed stronger staining, whereas chondrocytes treated with IL-1β showed weaker staining, suggesting TGF-β1 and IL-1β promote either synthesis or degradation of ECM, respectively. Within the TGF-β1 treated group, the strongest staining of ECM proteins was in chondrocytes on 90 kPa substrates; within the IL-1β treated group, the weakest staining of ECM proteins was in chondrocytes on 1 kPa substrates. This indicated that, with the substrate stiffness increasing from 1 to 90 kPa, the anabolic effect of TGF-β1 on ECM synthesis was enhanced and the catabolic effect of IL-1β weakened.

3.7. Changes of F-Actin and Focal Adhesion to Stretch. On the basis of the ECM staining results, we speculated that the altered ECM synthesis on PA substrates changed the attachment of chondrocytes to the substrate, which in turn affected the chondrocyte traction force. To test this hypothesis, we compared the responses of TGF-β1 or IL-1β treated chondrocytes while stretching the substrates. Using a

custom-built indentation system (Figure 7A), we applied a 15% strain to the PA substrates. Then we measured the stiffness of chondrocytes in the indenting region for 30 s, and fixed and stained chondrocytes for vinculin subsequently. As shown in Figure 7B, the TGF-β1 treated chondrocytes exhibited "strain-hardening" on 1 and 11 kPa substrates, as indicated by the increase of cellular stiffness, reflecting substrate strain transmitted to the actin cytoskeleton through focal adhesion of chondrocytes. However, the TGF-β1 treated chondrocytes on 90 kPa substrates showed a marked decrease in cellular stiffness, indicating that the cells might have received too much stress so that the cell−ECM coupling and the actin cytoskeleton were impaired or even damaged. Compared to the TGF-β1 treated cells, the IL-1β treated chondrocytes showed a consistent increase of cellular stiffness with increasing substrate stiffness from 1 to 90 kPa (Figure 7B). These results indicated that the stress transmission from the substrates to the IL-1β treated chondrocytes was not as efficient as to TGF-β1 treated chondrocytes. The treatment of IL-1β for 24 h reduced the deposition and distribution of major ECM components type II collagen and aggrecan (Figure 6, IL-1β). The disruption of ECM thus provided fewer contacting sites for chondrocytes and led to a poor cell−ECM−substrate attachment. Therefore, when a substrate strain was applied, some IL-1β treated chondrocytes (or some regions within a single cell) with poor ECM attachment were less influenced. This was further confirmed by the results of vinculin staining (Figure 7C). Generally, as compared to the unstretched chondrocytes, chondrocytes in the stretched region showed disturbed or even disrupted vinculin staining structure in all cases. However, the TGF-β1 treated chondrocytes showed a greater disturbance in vinculin than IL-1β treated chondrocytes after the stretch, indicating the former cells were more strongly attached to the substrate.

4. DISCUSSION

A growing body of evidence has revealed that physical properties of ECM affect and even control cell behaviors. As such, cell−ECM physical interaction has been a focus in cell mechanics (cellular level) and tissue engineering (tissue level) over the past decade, with the wide application of substrates (in vitro) and scaffolds (in vivo) having mechanical properties similar to those of the native ECM.[31] Here, we used PA gel as a model system to study the mechanical interaction between chondrocytes and substrate. Since synthetic PA substrate does not offer biological sites for cell attachment, the coating of ECM ligand to the substrate surface is necessary. A previous study has shown that chondrocytes exhibit very similar morphologies, gene expression, matrix formation, and cytoskeletal organization on plastic dishes coated with fibronectin, or type I collagen, or type II collagen,[32] indicating no particular preference of chondrocytes to these ECM ligands in vitro. Therefore, in this study, we did not examine the effects of different ECM coatings on chondrocyte−substrate interaction, but instead simply chose type I collagen as the adhesive ligand. In determining the stiffness of a substrate, we used PA gel with a Young's modulus of 1 kPa to mimic an ECM softer than normal chondrocyte pericellular matrix (PCM)[33] in vivo (note that 1 kPa is even smaller than the reported stiffness of chondrocytes from large animals[34,35]), we used 11 kPa gel to mimic an ECM which is in the stiffness range of PCM, and we used 90 kPa gel to mimic an ECM which is stiffer than PCM but softer than the native ECM.[36] We found that the spreading and SF formation were enhanced as substrate stiffness increased from 1 to 90 kPa, which is consistent with a previous study by Schuh et al.[16] that reports promoted spreading, SF organization, and cell proliferation as PA substrate stiffness increases from 4 to 100 kPa. Note that chondrocytes on 4 kPa substrate in their study showed less spreading instead compared to chondrocytes on 1 kPa substrate in our study. The difference of these observations could be attributed to the variances in cell source, passage, culture medium, and ECM ligand density. In terms of ECM production, we found that the increase of substrate stiffness enhanced the fluorescent intensity of type II collagen and aggrecan, suggesting a promoted ECM synthesis. In contrast, Schuh et al. reported the best ECM production on 4 kPa substrate compared to stiffer substrates in their study. Moreover, Allen et al.[17] cultured chondrocytes on PA substrate with stiffness in the megapascal range, and found that the expression of Sox9, aggrecan, and type II collagen was higher on 0.5 MPa (close to the stiffness of native cartilage) than on 1.1 MPa (stiffer) or 0.2 MPa (softer). Although these observations are not completely consistent with each other, we speculate that the chondrogenic effect of substrate/scaffold increases when its stiffness approaches the stiffness of native cartilage and decreases when its stiffness deviates from the stiffness of native cartilage.

However, the combinatory effects of ECM elasticity and biochemical factors on chondrocyte behavior remain less understood. Among the numerous signaling molecules, TGF-β1[37] and IL-1β[38] have emerged as the most critical anabolic factor and catabolic factor, respectively, in chondrocyte and cartilage pathophysiology. IL-1β is markedly expressed in osteoarthritic cartilage, which not only suppresses chondrocyte ECM synthesis but also stimulates the release of catabolic proteases, whereas, TGF-β1 does the opposite: it stimulates ECM production and promotes the chondrogenic phenotype. For this reason, in this study we investigated the mechanoresponses of chondrocytes to substrate elasticity in the presence of TGF-β1 or IL-1β.

First, we measured the cellular stiffness of chondrocyte. Chondrocyte stiffness is thought to be largely dependent on actin SFs,[39] and the amount of SFs has been shown to impact the chondrocyte phenotype: the presence of abundant SFs is associated with a reduction of type II collagen and aggrecan,[40] while disruption of SFs restored the production of type II collagen and aggrecan.[41] Moreover, chondrocyte stiffness significantly decreases with ECM degradation in cartilage diseases such as osteoarthritis (OA).[42] These observations suggest that chondrocyte stiffness is closely related to cartilage physiology. Here we found that both TGF-β1 and IL-1β increased chondrocyte stiffness, with TGF-β1 most effective on 90 kPa substrates (Figure 2C) and IL-1β most effective on 1 kPa substrates (Figure 2D). Interestingly, for the nontreated chondrocytes, the increase of cell stiffness by increasing the substrate stiffness enhanced SFs (Figure 1B) but still promoted the production of type II collagen and aggrecan (Figure 6), which is different from the previous finding.[40] The difference might result from the different stiffnesses of substrates used. For TGF-β1 or IL-1β treated chondrocytes, the increase of cellular stiffness reflects the upregulation of actin cytoskeleton resulting from the combinatory effects of substrate stiffness and soluble chemical factors via Rho/ROCK. The Rho/ROCK pathway has been shown to play an important role in actin assembly, focal adhesion formation, and even the cellular mechanosensing of ECM elasticity.[43,44] Particularly in chon-

drocytes, the Rho/ROCK pathway regulates actin dynamics and SF organization,[45,46] which in turn regulates chondrocyte differentiation and the chondrogenic phenotype. The level of actin in chondrocytes grown on tissue culture plastic inhibits chondrogenesis,[45] while the level of actin in chondrocytes grown on compliant substrates promotes chondrogenesis.[17] The regulation of the actin level becomes more complex in the presence of soluble factors: as we showed here the prochondrogenic TGF-β1 was most effective on 90 kPa substrates (Figure 2C) but the antichondrogenic IL-1β was most effective on 1 kPa substrates (Figure 2D) to increase cellular stiffness, indicating that the regulation of actin level through ROCK was more effective on stiff or soft substrate, respectively, for TGF-β1 treated or IL-1β treated chondrocytes. Therefore, further studies are needed to elucidate the mechanism of ROCK regulation in response to a combination of ECM elasticity and biochemical factors.

Second, we measured the traction forces of chondrocytes. Traction force shows the adhesive strength between the cell and its substrate, and plays key roles in cell adhesion and migration. To our knowledge, this is the first study that reports traction forces of chondrocytes. Chondrocytes in vivo are surrounded and protected by PCM and ECM; thus they are not as motile and contractile as many other tissue cells. Here we showed that both the nontreated single chondrocytes (Figure 3A, top) and chondrocyte monolayer (Figure 4A, top) exhibited steady adhesion strength and force distribution, indicating a relatively static condition of the cells if no mechanical perturbation is applied. Moreover, in a chondrocyte monolayer, the traction mainly arises from cell−substrate adhesion, and the tractions in cell−cell junctions were almost negligible. This observation was also expected, as chondrocytes in vivo are sparsely distributed and no cell−cell communication is needed to fulfill their task.

For the TGF-β1 treated chondrocytes, their traction forces increased more on 11 and 90 kPa substrates than on 1 kPa substrates (Figures 3B and 4B), while for the IL-1β treated chondrocytes, their traction forces decreased more on 1 kPa substrates than on 11 and 90 kPa substrates (Figures 3C and 4C). These changes of chondrocyte traction forces were actually shown to be related to the effects of TGF-β1 and IL-1β on ECM synthesis. The presence of TGF-β1 not only promoted focal adhesion and SF formation, but also enhanced chondrocyte ECM by stimulating the synthesis of type II collagen and aggrecan (Figure 6, middle). Both effects became more potent as substrate stiffness increased; therefore, the traction forces of TGF-β1 treated chondrocytes were higher on 11 and 90 kPa substrates than on 1 kPa substrates. In contrast, although the presence of IL-1β also increased the chondrocyte stiffness as TGF-β1 did, it degraded the ECM layer on PA substrates (Figure 6, right). The ECM degradation led to poor cell−ECM−substrate adhesion. As can be seen in the traction map (Figure 3, bottom), the single chondrocyte treated with IL-1β exhibited a narrowing force distribution, indicating reduced adhesion sites to the substrate. The effect of IL-1β on ECM synthesis was most obvious on 1 kPa substrates, and the weakest cell−substrate attachment induced the smallest traction force, although the percentage of stiffness increase of IL-1β treated chondrocytes was highest on 1 kPa substrates (Figure 2D). Generally, a change of cell traction forces is associated with a change of cellular stiffness, as stiffer cells generate bigger traction forces. Wang et al. used a panel of drugs to regulate the cytoskeletal tension of human airway smooth muscle cells, and found that traction forces changed in proportion to cellular stiffness.[47] Similarly, in our study, both traction forces (Figures 3B,C and 4B,C) and cellular stiffness (Figure 1E) increased along with the increase of substrate stiffness.

Finally, we measured chondrocyte responses to a mechanical stretch. Articular chondrocytes in vivo are subjected to mechanical forces such as compression during their lifetime, and such mechanical forces play an important role in regulating chondrocyte function.[48] Abnormal responses to mechanical forces can alter chondrocyte metabolism and therefore lead to joint degeneration such as OA.[49] Here we showed that TGF-β1 treated chondrocytes might have received bigger stress from the substrate stretch than IL-1β treated chondrocytes did, as indicated by the changes of cellular stiffness (Figure 7B) and vinculin focal adhesion (Figure 7C). However, chondrocytes in load-bearing joints are typically subjected to compression rather than stretch. Our results in turn suggested that the increasing ECM stiffness and the presence of TGF-β1 would promote cell−substrate adhesion and help chondrocyte deformation and mechanotransduction in response to joint loading.[50] However, we were unable to measure the changes of traction force during stretch because the substrate strain changed the displacement of the embedded fluorescent beads; we did not stain the actin after the stretch because the actin cytoskeleton can experience quick remodeling and reorganization to adjust the cytoskeletal tension and cellular stiffness back to the prestretch level.[51]

Overall, our results reveal that the presence of soluble factor (chemical signal) TGF-β1 and IL-1β affects chondrocyte mechanoresponses to substrate stiffness (mechanical signal) through regulating the signaling pathway (e.g., ROCK) and altering ECM−scaffold attachment. Because of the interaction between chemical and physical factors, a successful engineered cartilage cannot be achieved by focusing on biochemical or mechanical factors alone; instead, both factors should be fully considered. One limitation of this study is that the substrates we used are two-dimensional, which is different from the three-dimensional (3D) ECM environment in vivo. A practical reason for us not to use 3D substrates is that the quantification of cellular stiffness and traction force in 3D is less than perfect, although techniques that measure cells in 3D are emerging.[52,53] Nevertheless, our study may provide insights in cartilage tissue engineering. First, as cartilage repair usually takes place in an inflammatory microenvironment, the large amount of proinflammatory cytokines can counteract the chondrogenic effect of the tailor-made substrate/scaffold. As shown in Figure 6, although the increase of substrate stiffness alone promoted the chondrocyte phenotype, the presence of IL-1β counteracted the majority of this effect. Therefore, the use of chondrogenic factors such as TGF-β to offset the catabolic effects of inflammatory cytokines is necessary. Second, the mechanoresponses of chondrocytes such as cellular stiffness and traction forces alter in response to substrate elasticity, biochemical factors, and external forces. Thus, the design of a bioreactor should take into account the mechanical properties of the substrate/scaffold and the effects of soluble factors to make sure the mechanoresponses to the bioreactor do support chondrocyte adhesion and function. Third, the inflammatory environment of injured cartilage might hinder the chondrocyte attachment to the engineered substrate/scaffold in vivo, which in turn interferes with the mechanoresponses of chondrocytes. Therefore, one future direction of cartilage tissue engineering could be the design of a substrate/scaffold that also serves as a

delivery vehicle[54,55] of chondrogenic factors to ensure the adhesion interface between the cell and the substrate/scaffold.

5. CONCLUSION

In this study, we demonstrated the combinatory effects of substrate stiffness and soluble biochemical factors TGF-β1 and IL-1β on chondrocyte mechanoresponses. TGF-β1 increased cellular stiffness and the traction force, and was most potent in doing so on stiff substrates (90 kPa); IL-1β increased cellular stiffness but decreased the traction force, and was most potent in doing so on soft substrates (1 kPa). TGF-β1 also induced stronger responses of chondrocytes to mechanical stretch than IL-1β did. These changes were due to not only the changes of the actin cytoskeleton and focal adhesion, but also the changes of chondrocyte anabolic and catabolic activity. Our results indicate a link between soluble and mechanical factors in mediating chondrocyte mechanobiology. To regulate the mechanical behavior of chondrocytes and to create a chondrogenic ECM in vitro, a precisely controlled mechanical and biochemical environment is demanded.

AUTHOR INFORMATION

Corresponding Authors

*E-mail: cclljjff@gmail.com
*E-mail: jointsurgery@163.com.

Notes

The authors declare no competing financial interest.

ACKNOWLEDGMENTS

We thank Dr. Jeffery Fredberg at the Harvard School of Public Health for providing lab facilities, and we thank Dr. Myron Spector at Harvard Medical School for providing chondrocytes. This work was supported by the National Natural Science Foundation of China Grants (31130021 and 31300773), China Postdoc Grant (2013M532152), and Chongqing Postdoc Grant (Xm201352).

REFERENCES

(1) Yim, E. K.; Darling, E. M.; Kulangara, K.; Guilak, F.; Leong, K. W. Nanotopography-Induced Changes in Focal Adhesions, Cytoskeletal Organization, and Mechanical Properties of Human Mesenchymal Stem Cells. *Biomaterials* **2010**, *31*, 1299−1306.

(2) Seidi, A.; Sampathkumar, K.; Srivastava, A.; Ramakrishna, S.; Ramalingam, M. Gradient Nanofiber Scaffolds for Tissue Engineering. *J. Nanosci. Nanotechnol.* **2013**, *13*, 4647−4655.

(3) Chen, W.; Weng, S.; Zhang, F.; Allen, S.; Li, X.; Bao, L.; Lam, R. H.; Macoska, J. A.; Merajver, S. D.; Fu, J. Nanoroughened Surfaces for Efficient Capture of Circulating Tumor Cells without Using Capture Antibodies. *ACS Nano* **2013**, *7*, 566−575.

(4) Feng, C. H.; Cheng, Y. C.; Chao, P. H. The Influence and Interactions of Substrate Thickness, Organization and Dimensionality on Cell Morphology and Migration. *Acta Biomater.* **2013**, *9*, 5502−5510.

(5) Gilbert, P. M.; Havenstrite, K. L.; Magnusson, K. E.; Sacco, A.; Leonardi, N. A.; Kraft, P.; Nguyen, N. K.; Thrun, S.; Lutolf, M. P.; Blau, H. M. Substrate Elasticity Regulates Skeletal Muscle Stem Cell Self-Renewal in Culture. *Science* **2010**, *329*, 1078−1081.

(6) Discher, D. E.; Janmey, P.; Wang, Y. L. Tissue Cells Feel and Respond to the Stiffness of Their Substrate. *Science* **2005**, *310*, 1139−1143.

(7) Pelham, R. J., Jr.; Wang, Y. Cell Locomotion and Focal Adhesions Are Regulated by Substrate Flexibility. *Proc. Natl. Acad. Sci. U. S. A.* **1997**, *94*, 13661−13665.

(8) Lo, C. M.; Wang, H. B.; Dembo, M.; Wang, Y. L. Cell Movement Is Guided by the Rigidity of the Substrate. *Biophys. J.* **2000**, *79*, 144−152.

(9) Engler, A. J.; Sen, S.; Sweeney, H. L.; Discher, D. E. Matrix Elasticity Directs Stem Cell Lineage Specification. *Cell* **2006**, *126*, 677−689.

(10) Benya, P. D.; Shaffer, J. D. Dedifferentiated Chondrocytes Reexpress the Differentiated Collagen Phenotype When Cultured in Agarose Gels. *Cell* **1982**, *30*, 215−224.

(11) Fragonas, E.; Valente, M.; Pozzi-Mucelli, M.; Toffanin, R.; Rizzo, R.; Silvestri, F.; Vittur, F. Articular Cartilage Repair in Rabbits by Using Suspensions of Allogenic Chondrocytes in Alginate. *Biomaterials* **2000**, *21*, 795−801.

(12) Mauck, R. L.; Soltz, M. A.; Wang, C. C.; Wong, D. D.; Chao, P. H.; Valhmu, W. B.; Hung, C. T.; Ateshian, G. A. Functional Tissue Engineering of Articular Cartilage through Dynamic Loading of Chondrocyte-Seeded Agarose Gels. *J. Biomech. Eng.* **2000**, *122*, 252−260.

(13) Wakitani, S.; Kimura, T.; Hirooka, A.; Ochi, T.; Yoneda, M.; Yasui, N.; Owaki, H.; Ono, K. Repair of Rabbit Articular Surfaces with Allograft Chondrocytes Embedded in Collagen Gel. *J. Bone Jt. Surg., Br. Vol.* **1989**, *71*, 74−80.

(14) Trappmann, B.; Chen, C. S. How Cells Sense Extracellular Matrix Stiffness: A Material's Perspective. *Curr. Opin. Biotechnol.* **2013**, *24*, 948−953.

(15) Fischer, R. S.; Myers, K. A.; Gardel, M. L.; Waterman, C. M. Stiffness-Controlled Three-Dimensional Extracellular Matrices for High-Resolution Imaging of Cell Behavior. *Nat. Protoc.* **2012**, *7*, 2056−2066.

(16) Schuh, E.; Kramer, J.; Rohwedel, J.; Notbohm, H.; Muller, R.; Gutsmann, T.; Rotter, N. Effect of Matrix Elasticity on the Maintenance of the Chondrogenic Phenotype. *Tissue Eng., Part A* **2010**, *16*, 1281−1290.

(17) Allen, J. L.; Cooke, M. E.; Alliston, T. ECM Stiffness Primes the TGFbeta Pathway to Promote Chondrocyte Differentiation. *Mol. Biol. Cell* **2012**, *23*, 3731−3742.

(18) Guilak, F. Biomechanical Factors in Osteoarthritis. *Best Pract. Res., Clin. Rheumatol.* **2011**, *25*, 815−823.

(19) Chen, C.; Krishnan, R.; Zhou, E.; Ramachandran, A.; Tambe, D.; Rajendran, K.; Adam, R. M.; Deng, L.; Fredberg, J. J. Fluidization and Resolidification of the Human Bladder Smooth Muscle Cell in Response to Transient Stretch. *PLoS One* **2010**, *5*, e12035.

(20) Capito, R. M.; Spector, M. Collagen Scaffolds for Nonviral IGF-1 Gene Delivery in Articular Cartilage Tissue Engineering. *Gene Ther.* **2007**, *14*, 721−732.

(21) Fabry, B.; Maksym, G. N.; Butler, J. P.; Glogauer, M.; Navajas, D.; Fredberg, J. J. Scaling the Microrheology of Living Cells. *Phys. Rev. Lett.* **2001**, *87*, 148102.

(22) Kasza, K. E.; Vader, D.; Koster, S.; Wang, N.; Weitz, D. A. Magnetic Twisting Cytometry. *Cold Spring Harb. Protoc.* **2011**, DOI: 10.1101/pdb.prot5599.

(23) Mijailovich, S. M.; Kojic, M.; Zivkovic, M.; Fabry, B.; Fredberg, J. J. A Finite Element Model of Cell Deformation During Magnetic Bead Twisting. *J. Appl. Physiol.* **2002**, *93*, 1429−1436.

(24) Han, S. K.; Colarusso, P.; Herzog, W. Confocal Microscopy Indentation System for Studying in situ Chondrocyte Mechanics. *Med. Eng. Phys.* **2009**, *31*, 1038−1042.

(25) Ohayon, J.; Tracqui, P. Computation of Adherent Cell Elasticity for Critical Cell-Bead Geometry in Magnetic Twisting Experiments. *Ann. Biomed. Eng.* **2005**, *33*, 131−141.

(26) Wang, J. H.; Lin, J. S. Cell Traction Force and Measurement Methods. *Biomech. Model. Mechanobiol.* **2007**, *6*, 361−371.

(27) Butler, J. P.; Tolic-Norrelykke, I. M.; Fabry, B.; Fredberg, J. J. Traction Fields, Moments, and Strain Energy That Cells Exert on Their Surroundings. *Am. J. Physiol.: Cell Physiol.* **2002**, *282*, C595−C605.

(28) Marinkovic, A.; Mih, J. D.; Park, J. A.; Liu, F.; Tschumperlin, D. J. Improved Throughput Traction Microscopy Reveals Pivotal Role for

Matrix Stiffness in Fibroblast Contractility and TGF-Beta Responsiveness. *Am. J. Physiol.: Lung Cell. Mol. Physiol.* **2012**, *303*, L169−L180.
(29) Wang, N.; Ostuni, E.; Whitesides, G. M.; Ingber, D. E. Micropatterning Tractional Forces in Living Cells. *Cell Motil. Cytoskeleton* **2002**, *52*, 97−106.
(30) Krishnan, R.; Park, C. Y.; Lin, Y. C.; Mead, J.; Jaspers, R. T.; Trepat, X.; Lenormand, G.; Tambe, D.; Smolensky, A. V.; Knoll, A. H.; Butler, J. P.; Fredberg, J. J. Reinforcement Versus Fluidization in Cytoskeletal Mechanoresponsiveness. *PLoS One* **2009**, *4*, e5486.
(31) Ross, A. M.; Jiang, Z.; Bastmeyer, M.; Lahann, J. Physical Aspects of Cell Culture Substrates: Topography, Roughness, and Elasticity. *Small* **2012**, *8*, 336−355.
(32) Brodkin, K. R.; Garcia, A. J.; Levenston, M. E. Chondrocyte Phenotypes on Different Extracellular Matrix Monolayers. *Biomaterials* **2004**, *25*, 5929−5938.
(33) Guilak, F.; Alexopoulos, L. G.; Upton, M. L.; Youn, I.; Choi, J. B.; Cao, L.; Setton, L. A.; Haider, M. A. The Pericellular Matrix as a Transducer of Biomechanical and Biochemical Signals in Articular Cartilage. *Ann. N.Y. Acad. Sci.* **2006**, *1068*, 498−512.
(34) Bader, D. L.; Ohashi, T.; Knight, M. M.; Lee, D. A.; Sato, M. Deformation Properties of Articular Chondrocytes: A Critique of Three Separate Techniques. *Biorheology* **2002**, *39*, 69−78.
(35) Knight, M. M.; van de Breevaart Bravenboer, J.; Lee, D. A.; van Osch, G. J.; Weinans, H.; Bader, D. L. Cell and Nucleus Deformation in Compressed Chondrocyte-Alginate Constructs: Temporal Changes and Calculation of Cell Modulus. *Biochim. Biophys. Acta* **2002**, *1570*, 1−8.
(36) Alexopoulos, L. G.; Williams, G. M.; Upton, M. L.; Setton, L. A.; Guilak, F. Osteoarthritic Changes in the Biphasic Mechanical Properties of the Chondrocyte Pericellular Matrix in Articular Cartilage. *J. Biomech.* **2005**, *38*, 509−517.
(37) Blaney Davidson, E. N.; van der Kraan, P. M.; van den Berg, W. B. TGF-Beta and Osteoarthritis. *Osteoarthritis Cartilage* **2007**, *15*, 597−604.
(38) Daheshia, M.; Yao, J. Q. The Interleukin 1beta Pathway in the Pathogenesis of Osteoarthritis. *J. Rheumatol.* **2008**, *35*, 2306−2312.
(39) Trickey, W. R.; Vail, T. P.; Guilak, F. The Role of the Cytoskeleton in the Viscoelastic Properties of Human Articular Chondrocytes. *J. Orthop. Res.* **2004**, *22*, 131−9.
(40) Mallein-Gerin, F.; Garrone, R.; van der Rest, M. Proteoglycan and Collagen Synthesis Are Correlated with Actin Organization in Dedifferentiating Chondrocytes. *Eur. J. Cell Biol.* **1991**, *56*, 364−373.
(41) Benya, P. D.; Brown, P. D.; Padilla, S. R. Microfilament Modification by Dihydrocytochalasin B Causes Retinoic Acid-Modulated Chondrocytes to Reexpress the Differentiated Collagen Phenotype without a Change in Shape. *J. Cell Biol.* **1988**, *106*, 161−170.
(42) Hsieh, C. H.; Lin, Y. H.; Lin, S.; Tsai-Wu, J. J.; Wu, C. H. H.; Jiang, C. C. Surface Ultrastructure and Mechanical Property of Human Chondrocyte Revealed by Atomic Force Microscopy. *Osteoarthritis Cartilage* **2008**, *16*, 480−488.
(43) Hall, A. Rho GTPases and the Actin Cytoskeleton. *Science* **1998**, *279*, 509−514.
(44) Ridley, A. J.; Hall, A. The Small GTP-Binding Protein Rho Regulates the Assembly of Focal Adhesions and Actin Stress Fibers in Response to Growth Factors. *Cell* **1992**, *70*, 389−399.
(45) Woods, A.; Wang, G.; Beier, F. RhoA/ROCK Signaling Regulates SOX9 Expression and Actin Organization During Chondrogenesis. *J. Biol. Chem.* **2005**, *280*, 11626−11634.
(46) Woods, A.; Beier, F. RhoA/ROCK Signaling Regulates Chondrogenesis in a Context-Dependent Manner. *J. Biol. Chem.* **2006**, *281*, 13134−13140.
(47) Wang, N.; Tolic-Norrelykke, I. M.; Chen, J.; Mijailovich, S. M.; Butler, J. P.; Fredberg, J. J.; Stamenovic, D. Cell Prestress. I. Stiffness and Prestress Are Closely Associated in Adherent Contractile Cells. *Am. J. Physiol.: Cell Physiol.* **2002**, *282*, C606−C616.
(48) Chen, C.; Tambe, D. T.; Deng, L.; Yang, L. Biomechanical Properties and Mechanobiology of the Articular Chondrocyte. *Am. J. Physiol.: Cell Physiol.* **2013**, *305*, C1202−C1208.
(49) Smith, R. L.; Carter, D. R.; Schurman, D. J. Pressure and Shear Differentially Alter Human Articular Chondrocyte Metabolism: A Review. *Clin. Orthop. Relat. Res.* **2004**, S89−S95.
(50) Szafranski, J. D.; Grodzinsky, A. J.; Burger, E.; Gaschen, V.; Hung, H. H.; Hunziker, E. B. Chondrocyte Mechanotransduction: Effects of Compression on Deformation of Intracellular Organelles and Relevance to Cellular Biosynthesis. *Osteoarthritis Cartilage* **2004**, *12*, 937−946.
(51) Trepat, X.; Deng, L.; An, S. S.; Navajas, D.; Tschumperlin, D. J.; Gerthoffer, W. T.; Butler, J. P.; Fredberg, J. J. Universal Physical Responses to Stretch in the Living Cell. *Nature* **2007**, *447*, 592−495.
(52) Kural, M. H.; Billiar, K. L. Regulating Tension in Three-Dimensional Culture Environments. *Exp. Cell Res.* **2013**, *319*, 2447−2459.
(53) Hall, M. S.; Long, R.; Feng, X.; Huang, Y.; Hui, C. Y.; Wu, M. Toward Single Cell Traction Microscopy within 3D Collagen Matrices. *Exp. Cell Res.* **2013**, *319*, 2396−2408.
(54) Park, J. S.; Yang, H. N.; Woo, D. G.; Jeon, S. Y.; Park, K. H. SOX9 Gene Plus Heparinized TGF-Beta 3 Coated Dexamethasone Loaded PLGA Microspheres for Inducement of Chondrogenesis of hMSCs. *Biomaterials* **2012**, *33*, 7151−7163.
(55) Jeon, S. Y.; Park, J. S.; Yang, H. N.; Woo, D. G.; Park, K. H. Co-Delivery of SOX9 Genes and Anti-Cbfa-1 SiRNA Coated onto PLGA Nanoparticles for Chondrogenesis of Human MSCs. *Biomaterials* **2012**, *33*, 4413−4423.